

Clamped Part Influence on Load-Deformation Behavior of Reinforced Concrete Shear Walls under Cyclic Loading



Florian Meier and Harald Schuler*

FHNW University of Applied Sciences and Arts Northwestern Switzerland, Hofackerstrasse, Muttenz, Switzerland

Submission: July 04, 2024; **Published:** July 15, 2024

***Corresponding author:** Harald Schuler, FHNW University of Applied Sciences and Arts Northwestern Switzerland, Hofackerstrasse, Muttenz, Switzerland

Abstract

Load-deformation behavior is decisive for the effectiveness of stiffening walls under earthquake loads and RC shear walls are an important tool to resist these loads. However, deformations in these walls' clamping zones are usually not considered; their benefits and risks are neglected. Carrying out large-scale wall tests and using an optical measurement system for displacements show that more attention should be paid to the clamping zone. In particular, clamped wall part bending deformations, as well as sliding shear deformations, should also be considered. A separation of displacement components clearly shows that stiffening walls' clamping zones have a positive influence on load-deformation behavior due to flexure. At the same time, the clamping zone, especially for squat walls, carries the risk of sliding shear failure, which would lead to a premature loss of horizontal stability.

Keywords: Earthquake Analysis; RC Shear wall; Bending-shear Interaction; Deformation Components; Load-displacement Curve; Sliding Shear Failure

Introduction

Horizontal stabilization of multi-store reinforced concrete buildings against earthquake effects is, in most cases, achieved by walls or cores made of reinforced concrete. Cantilevered upper floors are stabilized by clamping in basement floors, with shear walls horizontally fixed by the basement ceiling and the floor slab (Figure 1). The wall section above the clamping horizon (ground floor upwards) is usually slender and is stressed primarily by bending. The wall section in basement floors is often squat. High shear and sliding shear stresses occur and interact with bending stresses.

Traditionally, such a stiffening wall was modeled as a cantilever arm with a clamping horizon at the basement ceiling. However, this approach does not take into account deformation capacity due to basement wall bending (clamping zone). Thus, total wall deformation may be underestimated and building deformability is not accurately assessed.

However, an additional failure mode is also neglected when the clamping zone is not considered. Sliding shear failure can

occur there because bending-induced crack opening reduces the wall's sliding shear resistance; as cyclic loading progresses, reinforcement is gradually exposed by bending and sliding shear stress, reducing shear transfer resistance across the crack. A sudden sliding failure in the construction joint below the basement ceiling can occur; then the clamping effect for the upper floors is lost. Compared to behavior under bending and shear conditions [1-4], there are far fewer studies on sliding shear behavior. Basic studies on sliding shear behavior of squat walls under cyclic action can be found in Syngé [5] and Luna et al. [6] and detailed studies on sliding failure in Trost et al. [7] and Schuler et al. [8].

To examine these different deformation components in more detail, a specially designed test rig was developed and set up. Deformations due to bending in cantilevered wall sections and to clamping area bending and sliding shear were examined separately. Shares of total deformation were worked out and clearly presented.

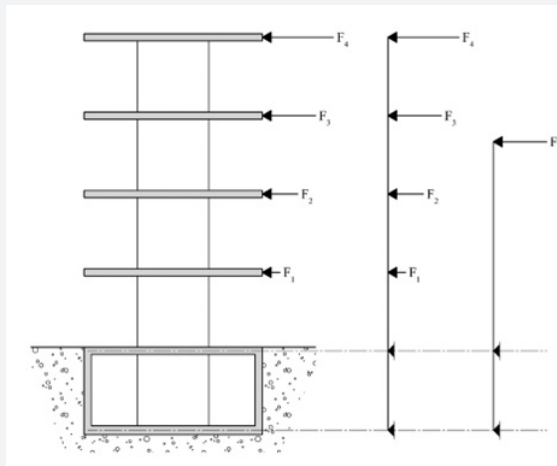


Figure 1: Reinforcement of a multi-store building: a) building model b) statical system c) simplified statical system according to a SDOF.

Test Setup

Test Stand and Load Application

The test stand was set up on the strong floor of the University of Applied Sciences Northwestern Switzerland construction laboratory. A recess in the strong floor made it possible to introduce horizontal forces from the test wall via the top and bottom of the strong floor. Horizontal supports consisted of a

reaction wall made of steel and concrete above and a steel shear wall below the strong floor (Figure 2). To minimize deformations of the supports themselves under the tests' great horizontal forces, the upper reaction wall and lower shear wall were pre-stressed vertically against each other through the strong floor. To transfer horizontal loads into the reaction wall, it was also pre-stressed horizontally.

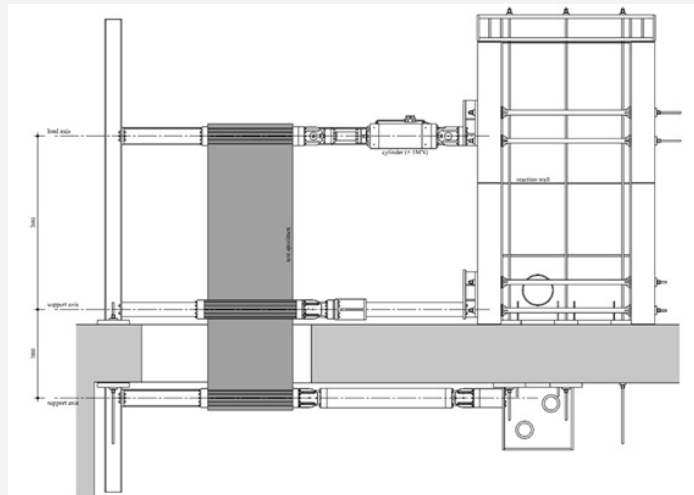


Figure 2: Side view of the test stand with the test specimen (in dark grey), strong floor, reaction wall (above) and steel shear wall (below).

The load axis was located around 4 m above the strong floor. The forces were applied to the test walls using a hydraulic cylinder (cylinder force +/- 1 MN). The cylinder had hinges at both ends to exclude flexural constraints when the top of the wall was rotating. The two bearing axes were located directly above and below the strong floor; these represented the bearings at the height of the basement ceiling and the floor slab in a real building and were also articulated (Figure 3).

Due to cyclic loading, the test walls were pressed against the hydraulic cylinder and support points - or pulled away from them - depending on load direction. To also transfer tensile forces, the test walls were clamped by pre-stressed rods and steel plates on the opposite side of the pressure points. The load was applied using a standardized procedure according to Park [9]; this was also used in comparable tests [2,3].

Test Specimens

Four test walls were examined, differing in geometry and reinforcement degree. Geometry and degree of reinforcement were chosen to correspond to typical walls found in actual construction. Wall 1 was a slender wall with a clamping area height-to-length ratio of 1 and a vertical reinforcement ratio of $\rho = 0.44\%$. Wall 2 had the same geometrical properties as Wall 1, but a higher vertical reinforcement ratio of $\rho = 2.23\%$ in the wall end zones ($0.15 l_w$). Wall 4 was more squat, with a clamping zone height-to-length ratio of about 0.75 and nearly the same vertical reinforcement ratio as Wall 1 ($\rho = 0.39\%$). All reinforcements ran continuously and were not overlapped. An overview of the geometries and reinforcement ratios of the test walls are given in Table 1.

h_{up} = Height of cantilever wall from the middle support axis to the upper load axis

h_{base} = Height of basement wall from the lower to the middle support axis

t = Wall thickness

l_w = Wall length

l_b = Length of reinforced boundaries

l_{web} = Length of web without boundaries

ρ_b = Boundary reinforcement ratio

ρ_{web} = Web reinforcement ratio

$\rho_{V,up}$ = Cantilever wall transverse reinforcement ratio

$\rho_{V,base}$ = Basement wall transverse reinforcement ratio

Wall 3 was a variant of test wall 1 with an external reinforcement. Retrofitted variants of the walls are not the topic of this publication.

Table 1: Shear wall geometry and reinforcement.

| Wall | h_{up} | h_{base} | t | l_b | l_{web} | ρ_b | ρ_{web} | $\rho_{V,up}$ | $\rho_{V,base}$ |
|------|----------|------------|-----|-------|-----------|----------|--------------|---------------|-----------------|
| | [m] | [m] | [m] | [m] | [m] | [%] | [%] | [%] | [%] |
| 1 | 3.68 | 1.86 | 0.2 | 0 | 1.8 | - | 0.44 | 0.39 | 0.39 |
| 2 | 3.68 | 1.86 | 0.2 | 0.27 | 1.26 | 2.23 | 0.44 | 0.39 | 0.79 |
| 4 | 3.68 | 1.86 | 0.2 | 0 | 2.4 | - | 0.39 | 0.39 | 0.79 |

Measurement Devices

Test wall deformations were recorded using an optical measuring system. For this purpose, a grid of self-adhesive reflectors was applied to the test walls in a uniform 20-cm grid vertically and horizontally over the entire wall surface. Each

reflector point was recorded by at least 3 cameras during the tests, from a total of 8 cameras, which allowed measurement of the coordinates in a three-dimensional space. The reflector points' coordinates from one point in time to the next allowed calculation of deformation increments, needed for the load-displacement curves.

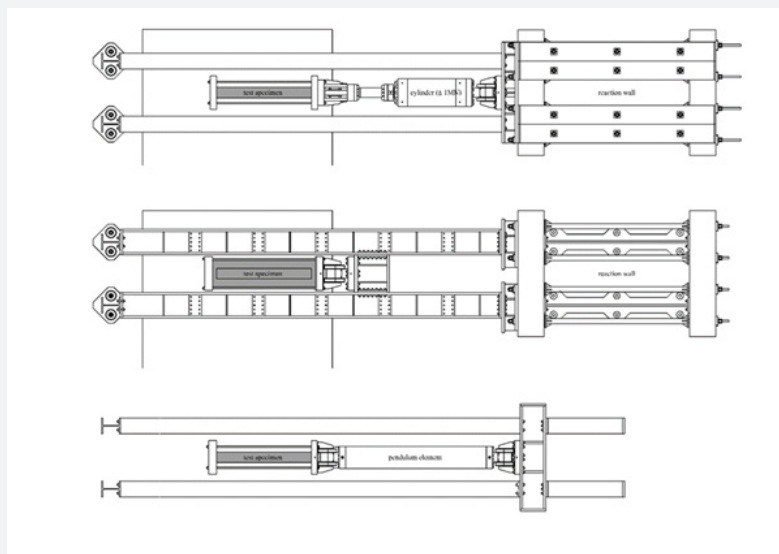


Figure 3: Floor plans of the test stand: a) load axis b) upper support axis c) lower support axis.

Examination of deformation components

A total of four deformation components occurred within the selected test setup: rigid body rotation, bending in the cantilevered wall part, bending in the clamping wall part and sliding in the construction joint between basement wall and ceiling cutout (Figure 4).

Because the rigid body rotation did not contribute to the internal deformations, it had to be calculated out.

To calculate rigid body rotation, rotated wall axis was determined for each measurement time. This was determined as a perpendicular to an average row of points from the first rows of points above and below the ceiling cutout (Figure 5 a). Two points were then determined on this inclined wall axis: top axis point TAP at the height of the load axis and the bottom axis point BAP at the height of the lower bearing axis. For these two points, the shift between two points in time was determined (Δu_{TAP} or Δu_{BAP}). These two shifts represent the wall top and wall bottom displacement increment due to rigid body rotation (Figure 5 b).

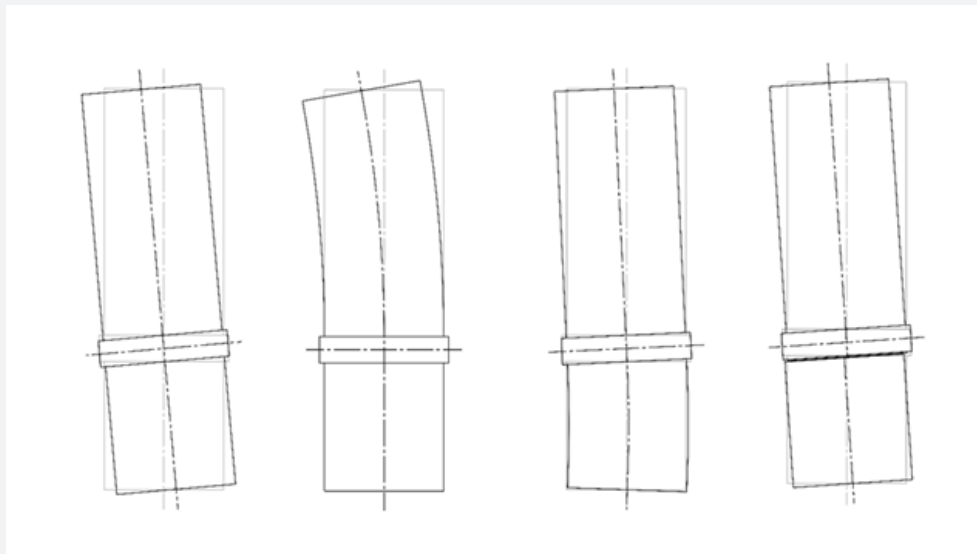


Figure 4: Deformation components: a) rigid body rotation b) bending in the cantilevered wall part c) bending in the clamping wall part d) sliding in the construction joint between the basement wall and the ceiling cutout.

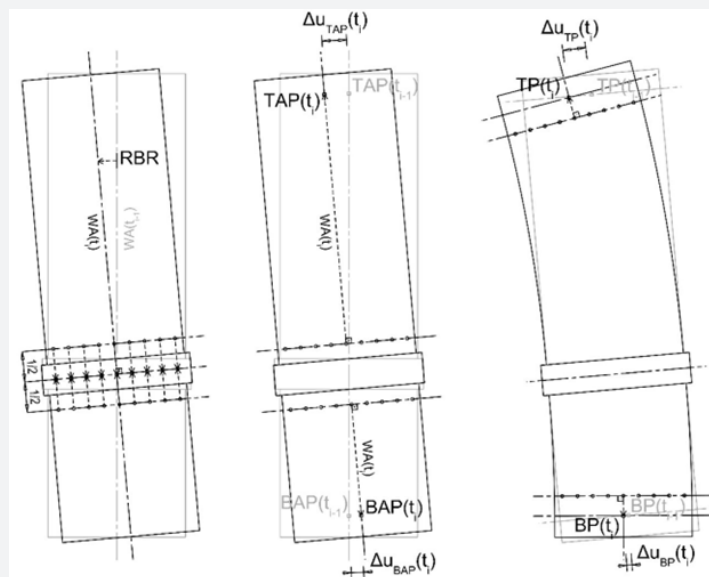


Figure 5: Rigid body rotation and bending: a) rotated wall axis b) shift of the top axis point TAP and bottom axis point BAP c) shift of the top wall point TP and bottom wall point BP.

Wall coordinates at the height of load axis TP were determined for each measurement time, using the top row of measuring points as shown in Figure 5c. For displacement increment between two measurement times, Δu_{TP} , the coordinate difference was calculated, which included rigid body rotation. To obtain the cantilevered wall part pure bending component from the total displacement Δu_{TP} , the rigid body rotation Δu_{TAP} was subtracted.

The same procedure was applied for the basement part of the wall, where the basement wall displacement increment, Δu_{BP} , was determined from the lowest row of measuring points. As before, for pure bending deformation, the portion from rigid body rotation Δu_{BAP} must be calculated out.

Sliding deformations were determined in two steps; first, centers of the first rows of points above and below the ceiling cutout $MP_{clamping}$ and $MP_{cantilever}$ were projected onto the center line of the ceiling cutout by right angles to the respective row of points: $MP'_{clamping}$ and $MP'_{cantilever}$ (Figure 6). Coordinate difference between two measurement times corresponds to the sliding displacement increment, which was calculated for the cantilevered and clamping wall parts, $\Delta u_{sliding,Cantilever}$ and $\Delta u_{sliding,Clamping}$.

The resulting sliding displacement increment $\Delta u_{sliding}$ was finally calculated by the difference between the two calculated sliding displacements (Figure 7). It must be mentioned; sliding only occurred on the construction joint below the ceiling cutout.

Test Results

Deformation Figures / Crack Patterns

Wall 1 showed a classic crack pattern dominated by bending (Figure 8a); first cracks appeared in the zone with the greatest bending moment, which opened successively with increasing load. Additional cracks developed along the wall height. The cracks ran horizontally, especially in the ends of the wall, and, as each became inclined, the closer they were to the pressure zone. As expected, the vertical spacing of the cracks corresponded to the horizontal reinforcement vertical spacing. The reinforcement weakened the tension zone, making cracking there more likely. Ultimately, the wall failed due to reinforcement breaking in the main crack immediately above the upper bearing axis. The maximum crack opening of the main crack was over 3 cm.

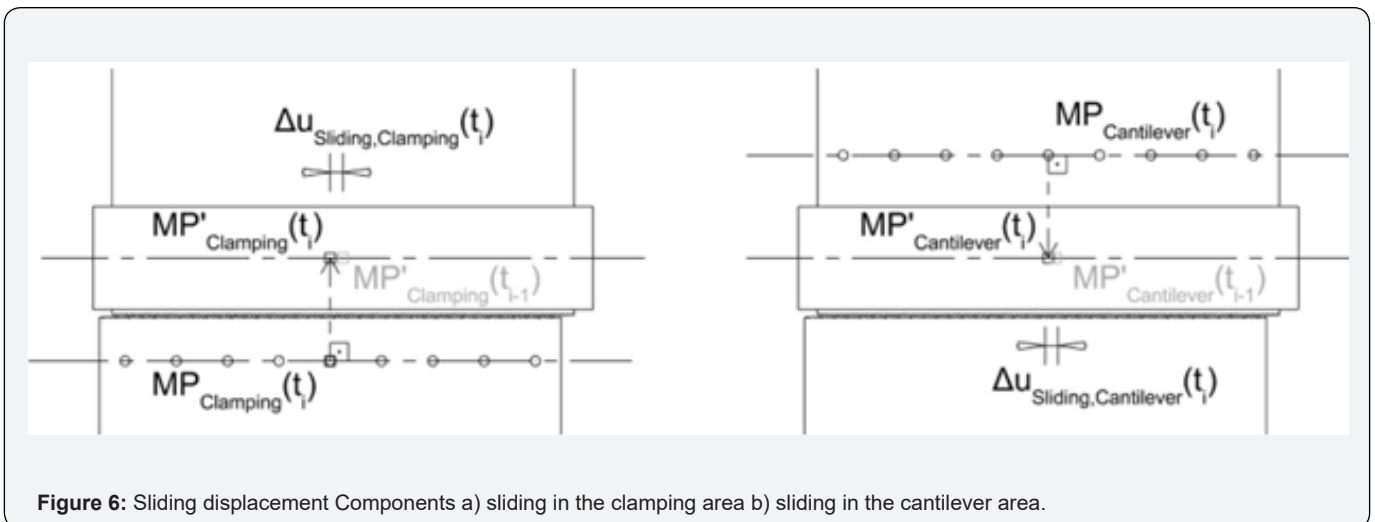


Figure 6: Sliding displacement Components a) sliding in the clamping area b) sliding in the cantilever area.

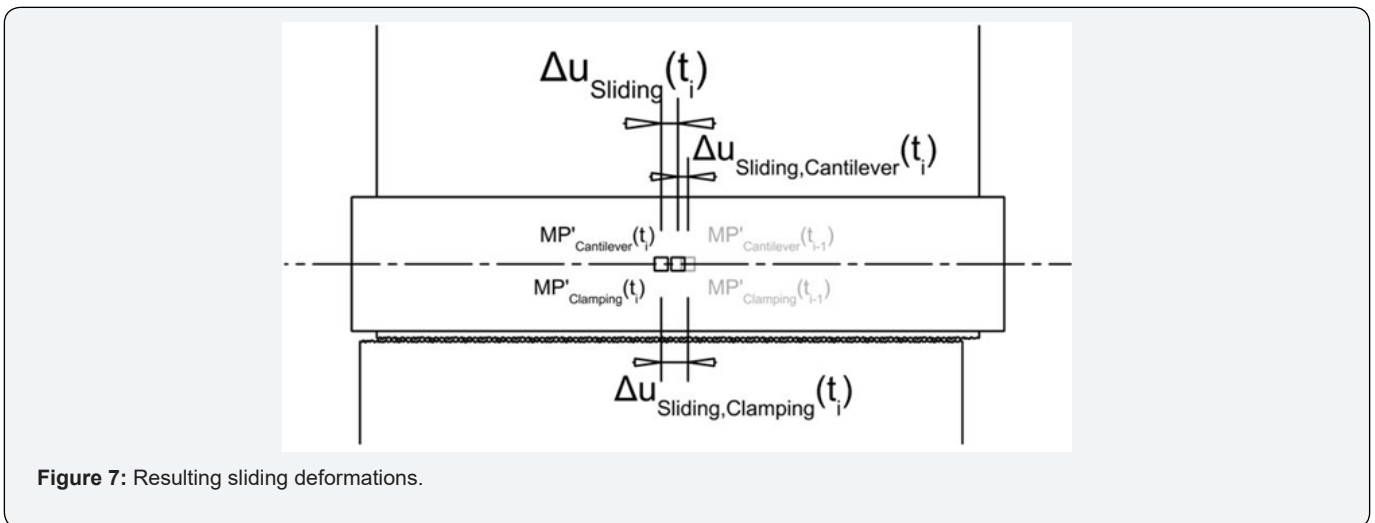


Figure 7: Resulting sliding deformations.

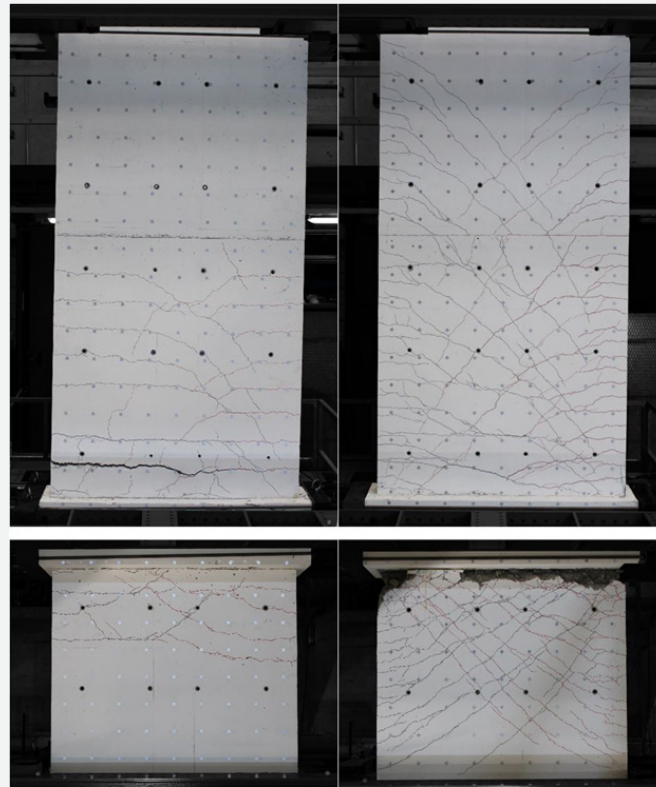


Figure 8: Crack patterns after completion of the experiment: a) Wall 1 b) Wall 2.

In contrast, Wall 2 showed a crack pattern characterized by a greater influence of shear forces (Figure 8b). Except in the edge zones with reinforced boundaries, the cracks showed a long-inclined part; an actual main crack could not be identified. Vertical crack spacings were smaller, in the edge zones, and followed the distance of the stirrups there. Especially in the lower wall section, between the two bearing axes, the crack pattern was dominated by the shear forces. As the load intensity increased, a horizontal sliding crack developed immediately at the transition from the lower wall section to the thickened element at the upper support axis (basement ceiling cutout). After this crack had completely formed, top displacement of Wall 2 resulted almost exclusively from sliding in the construction joint; other cracks opened only slightly. Deformations in this sliding crack increasingly eroded the concrete and completely exposed the reinforcement. Ultimately, weak vertical reinforcement between edge zones failed in the sliding crack due to shearing, so that further loading of the test wall was no longer possible.

Wall 4 showed a very differentiated crack pattern, which additionally depended on loading direction (Figure 9); in one loading direction (load to the north), cracks in areas with high moment loads ran mainly horizontally. Higher up the wall, where shear force became more dominant compared to the moment, the cracks had definitive inclination and ran horizontally over a

shorter length at the wall ends. Few cracks occurred in the lower wall section (clamping part) under this loading direction. For the other loading direction (to the south), the opposite crack pattern occurred: only a few horizontal cracks formed in the wall's upper section, but more cracks appeared in its lower section. This asymmetry can be explained by the vertical wall support, located north of the upper support axis. In the upward cantilevering part, an additional compressive force from the hydraulic cylinder dead weight was evident. In the lower clamping part, there was an additional tensile force from the ram in the lower support axis.

With Wall 4, a horizontal sliding crack developed directly at the transition from the lower wall section to the ceiling cutout, but at an earlier load stage than for Wall 2. In addition, the abrasion of the concrete was less pronounced.

Total top displacement

Since the test walls' support on the bearing axes was significantly stiffer in compression than in tension, system stiffness depended on the load direction. As a result, a larger overall deformation for loads to the north was measured in all wall tests (Figure 10, Figure 11 & Figure 12).

All tests also showed that the maximum force in the second cycle of a load stage was smaller than in the first cycle, with a reduction between 10% and 30%.

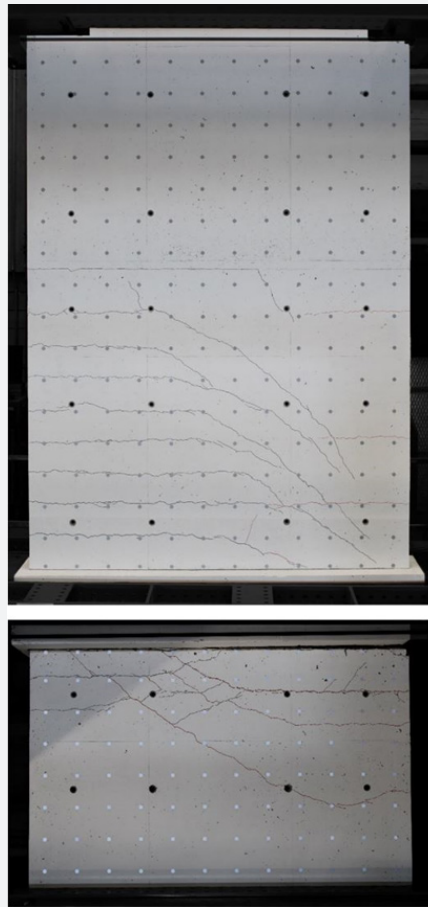


Figure 9: Crack patterns after completion of the experiment: Wall 4.

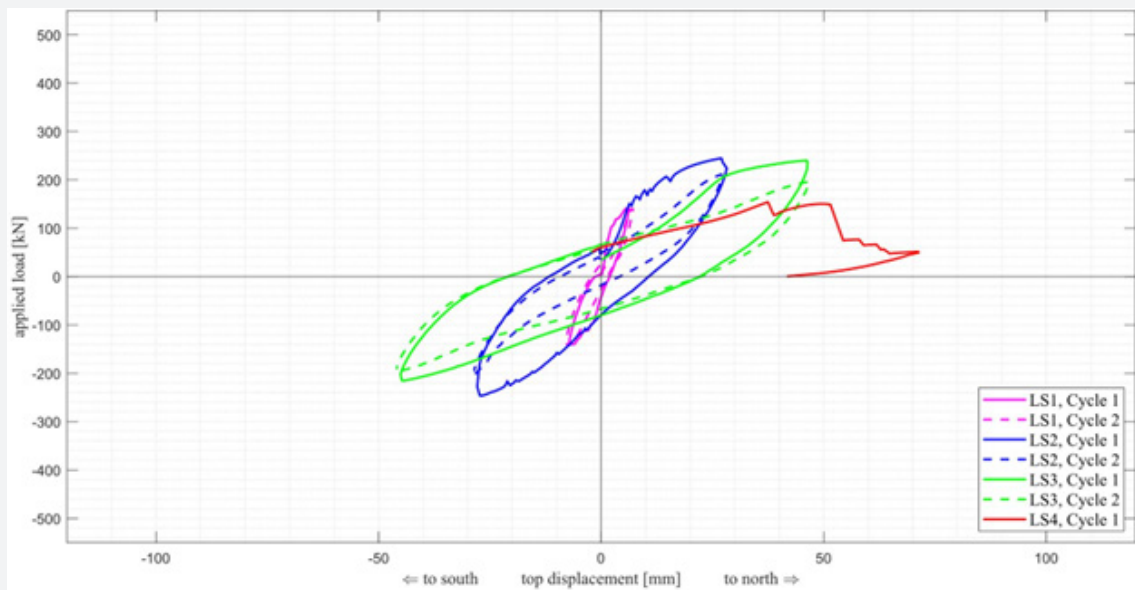


Figure 10: Total top displacement Wall 1.

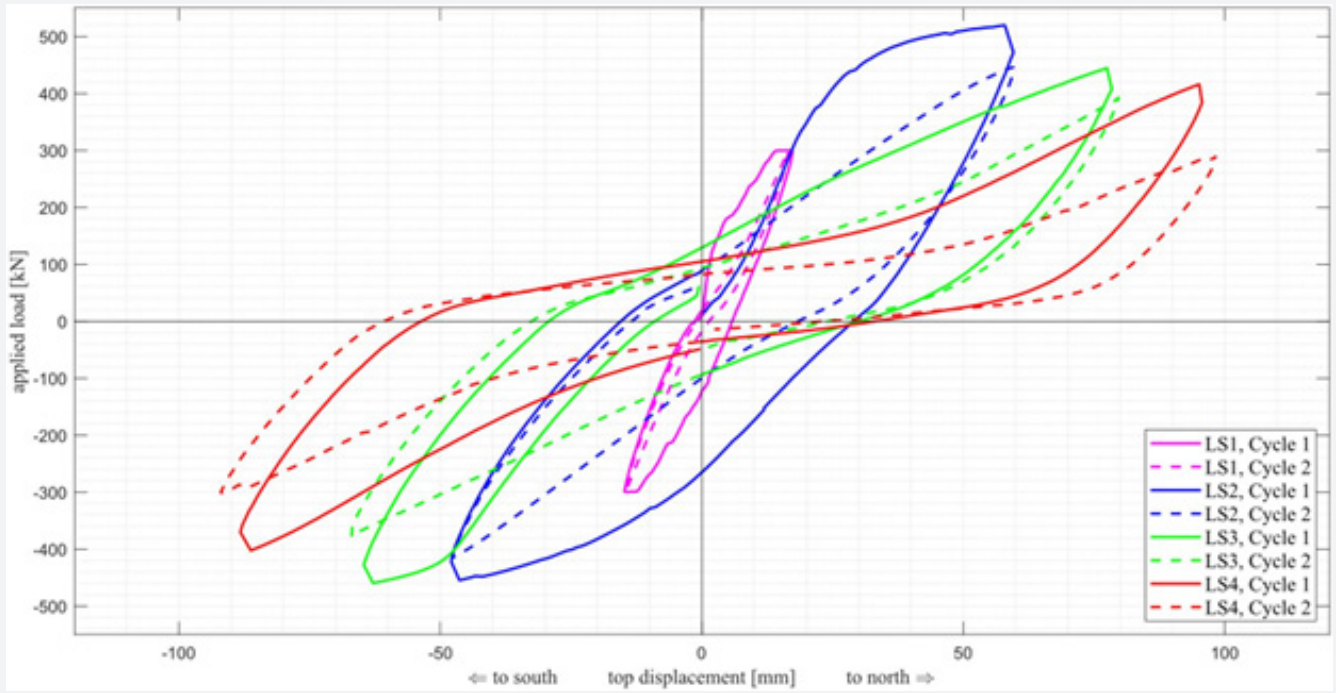


Figure 11: Total top displacement Wall 2.

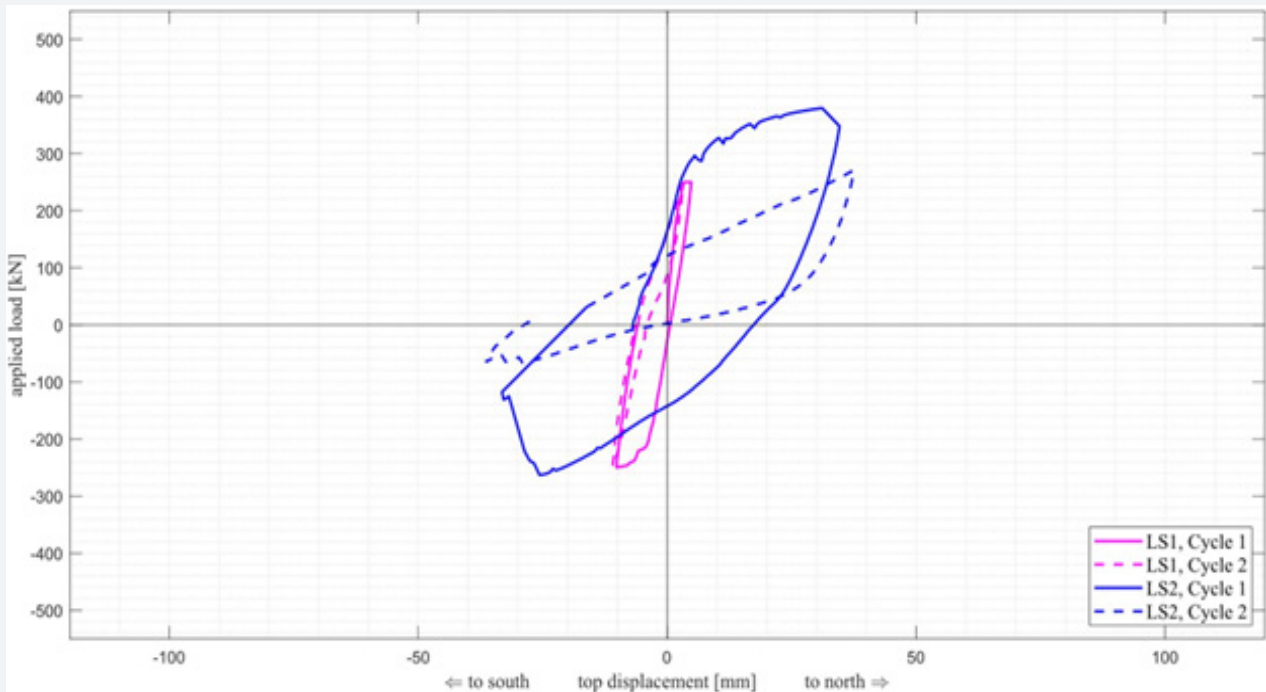


Figure 12: Total top displacement Wall 4.

Wall 1 reached a maximum load of around 240 kN in load stage 2 and a maximum total deformation of around 50 mm in load stage 4. The great load drop only occurred in the last cycle (Figure 10).

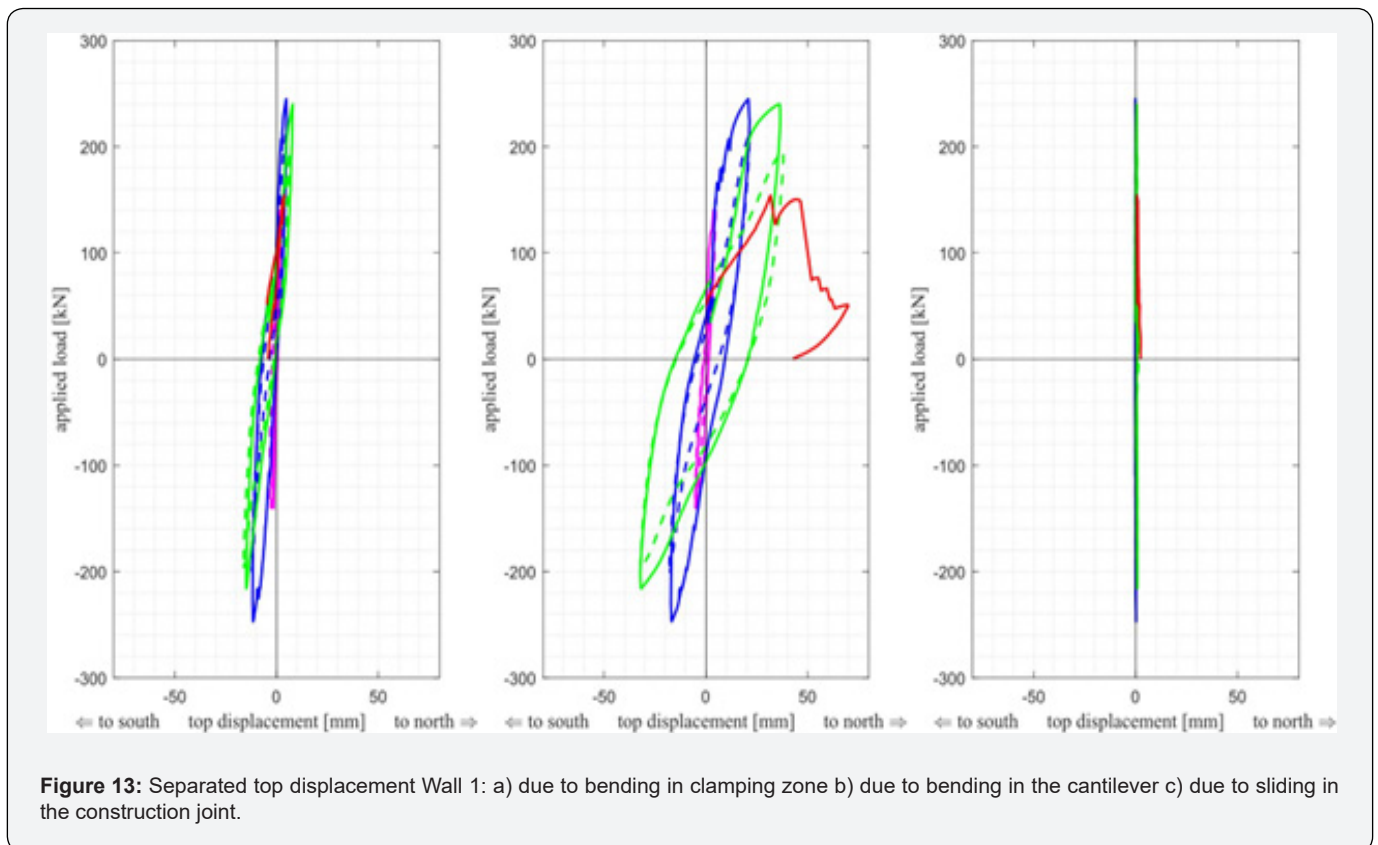
Wall 2 could be loaded up to 520 kN (load level 2), which corresponded to a load increase of 117% compared to Wall 1. At just under 100 mm, total deformation could not be quite doubled compared to Wall 1. The load-deformation curve of Wall 2 shows the switch in deformation behaviour very clearly from bending (load stage 1 and 2) to sliding (partial load stage 3 and particularly in load stage 4); The initially stiff deformation behavior under bending gradually changed to a very soft behavior when sliding occurred. Especially in load stage 4, it can be seen how the test wall underwent large deformations without experiencing a significant increase in load. In this stage, the load-deformation curve was almost horizontal in the inner part of Figure 11.

Wall 4 reached a maximum load of 380 kN and could thus

absorb around 58% more load than Wall 1 and around 27% less than Wall 2. The maximum total deformation of 38 mm was, however, significantly below the values of the first two test walls with 50 mm (Wall 1, - 24%) or 100 mm (Wall 2, - 62%). The increase in stiffness was because of the wall's greater length (1.5 times greater than in Wall 1 and Wall 2). Sliding displacements already occurred in the Wall 4 in the second load cycle of stage 2 (Figure 12).

Separated Top Displacement

Breaking down displacements into three components (bending in the clamping zone, bending in the cantilever, and sliding), the three test walls showed very different behaviors: total displacement of Wall 1 was dominated by bending deformation in the cantilever for both loading directions (Figure 13b). Displacements resulting from the clamping part were rather small (Figure 13a) and displacements from sliding shear occurred negligibly (Figure 13c).



Wall 2 experienced a larger proportion of total displacements from the clamping part (Figure 14a), whereby here, as with Wall 1, proportion for the load to the south was more pronounced. Cantilever bending deformation dominated total deformation of Wall 2 for the first two load stages, but from the third load stage onward, this increased only to a small extent (Figure 14b). Observed sliding failure of Wall 2 was also clear in the proportion of the displacement from sliding shear to the total displacement.

Initially, displacements from sliding shear were small, but continuously increased from load stage 3 and became dominant until failure (Figure 14c). Displacements from sliding shear not only increased from load stage to load stage, but also from the first cycle to the second cycle within one load stage.

Total displacements of Wall 4 are highly differentiated. While clamped part bending displacements accounted for the largest share of the load to the south, especially in the first cycle of load

stage 2, cantilever bending displacements were decisive for the load to the north (Figure 15a & Figure 15b). Initially, sliding deformations only occurred to a small extent in Wall 4, but

increased sharply in the second cycle of load stage 2 and, together with the cantilever bending deformation, accounted for the test wall's total deformation.

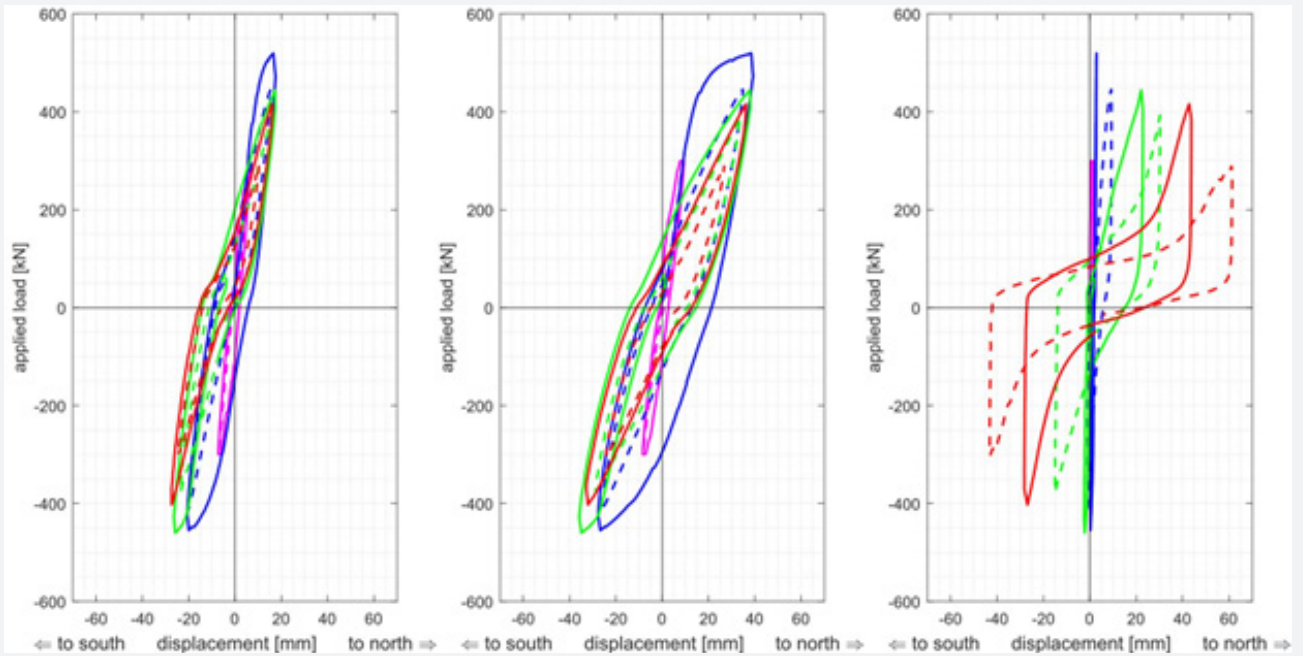


Figure 14: Separated top displacement Wall 2: a) due to bending in clamping zone b) due to bending in the cantilever c) due to sliding in the construction joint.

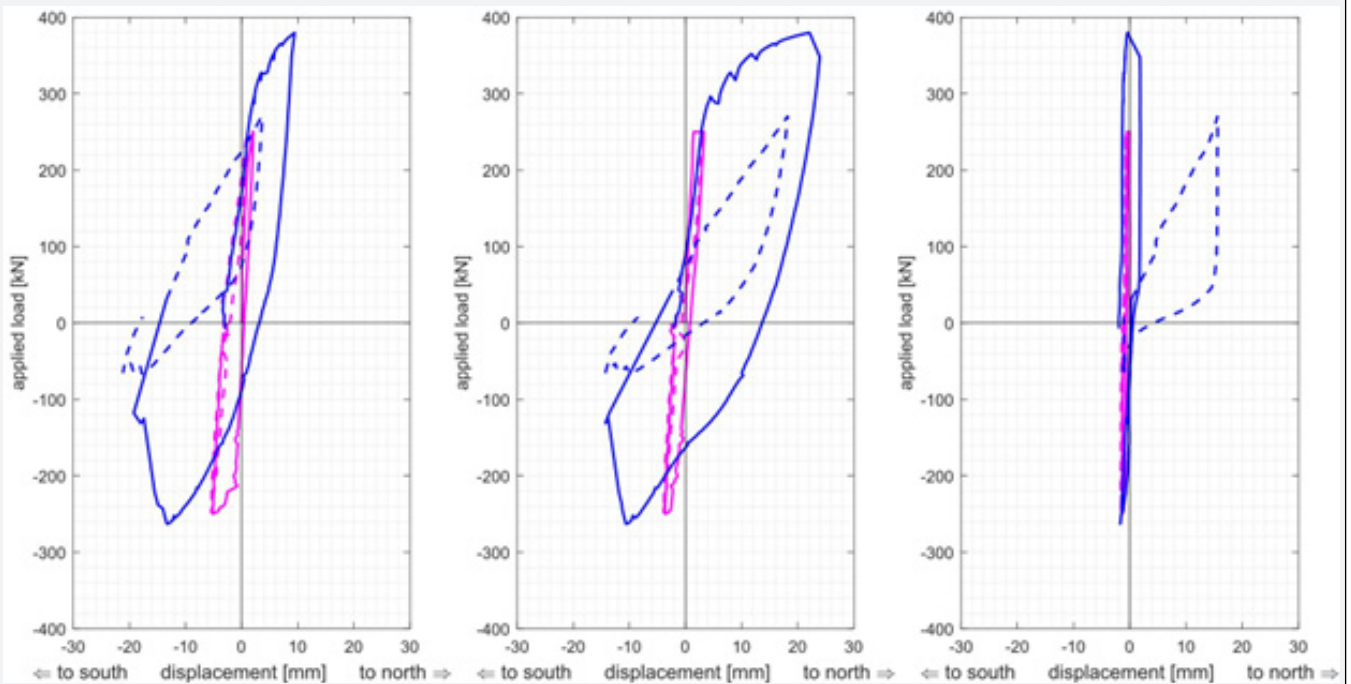


Figure 15: Separated top displacement Wall 4: a) due to bending in clamping zone b) due to bending in the cantilever c) due to sliding in the construction joint.

Relative Displacement Components

If one looks at the three deformation components' percentage distribution at the maximum load of each load stage, previous observations were confirmed. The total displacement of Wall 1 resulted mainly from bending deformation in the cantilevered part of the wall, which was slightly more dominant for the loading

to the north (68% to 84% of the total displacement) than for south loading (59% to 73% of the total displacement) in the first cycles. The second cycles showed nearly the same characteristics (Figure 16 and Figure 17). The pure bending behavior of Wall 1 was also reflected in the very small proportion of displacements of sliding shear (less than 2%) across all load stages and load cycles.

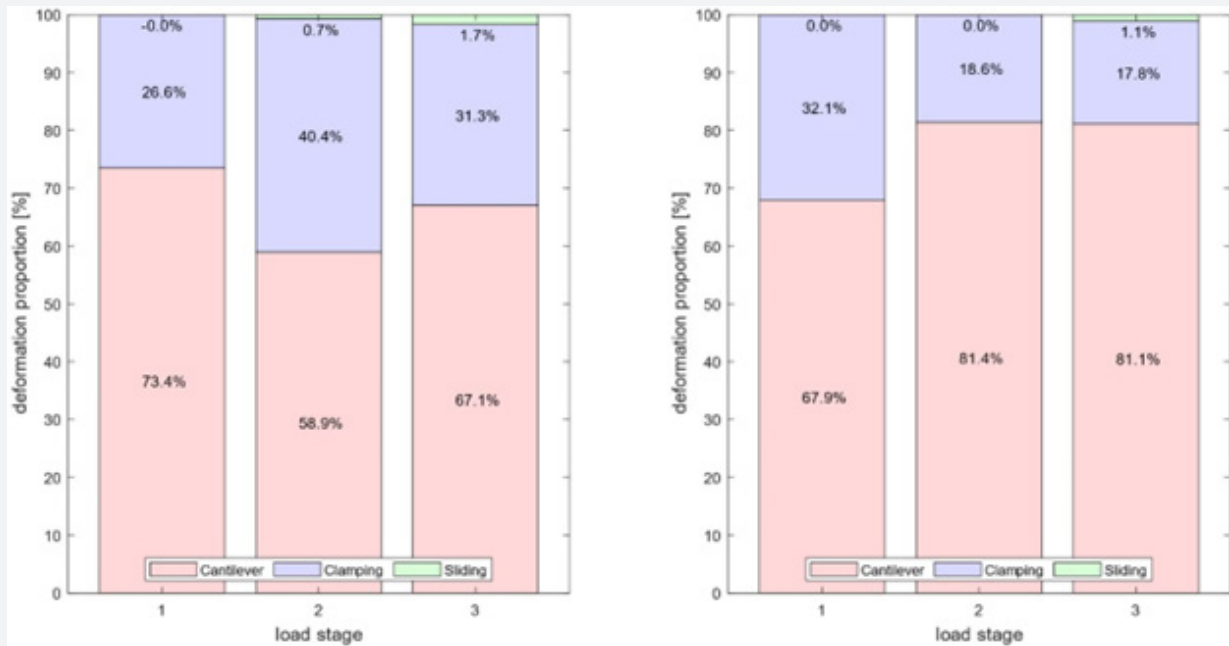


Figure 16: Relative displacement components of Wall 1, first loading cycles: a) loading to south b) loading to north.

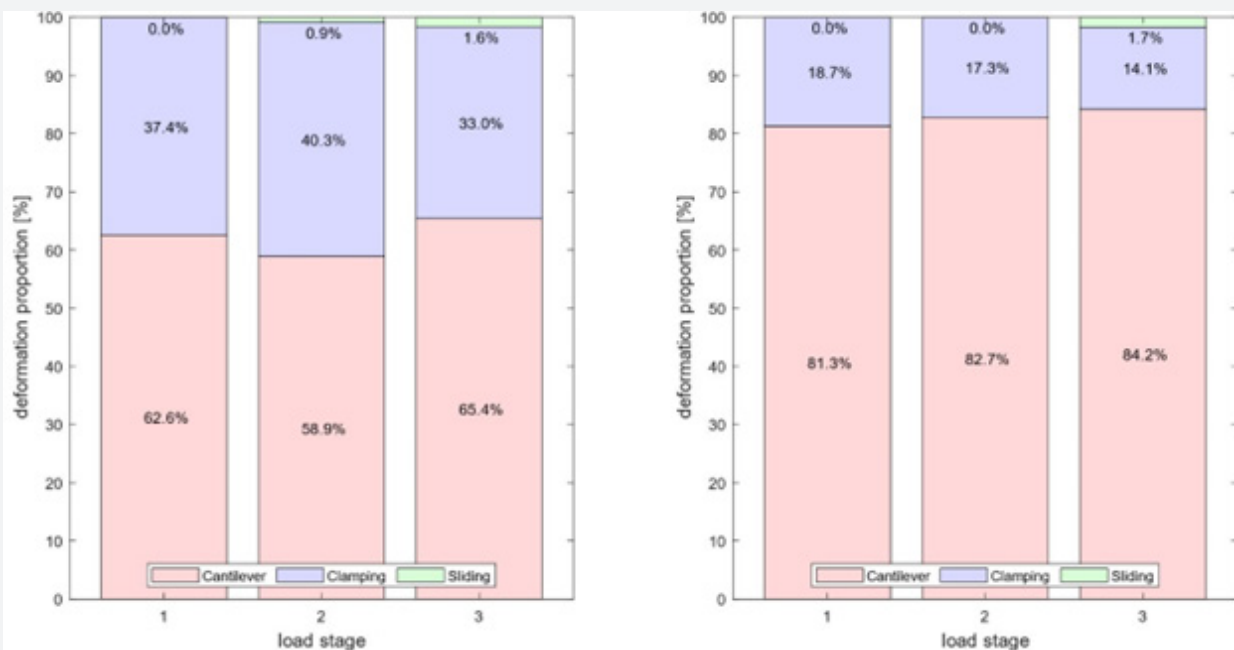


Figure 17: Relative displacement components of Wall 1, second loading cycles: a) loading to south b) loading to north.

The later sliding shear failure of Wall 2 was already apparent in the first load stage, at least for the load to the north. In first and second load cycle (Figure 18 & Figure 19), proportion of displacement from sliding shear was already around 10% of the total. Except for the first cycle in load stage 2, this proportion increased continuously with each additional load stage and reached a proportion of 62% in the last load stage. The same behavior, although less pronounced, could be seen for the load

to the south. It was also noticeable that bending proportions decreased to varying degrees. While cantilever part bending decreased from around 54% -> 38% / 54% -> 37% (first load cycle north / south) resp. from 54% -> 27% / 54% -> 26% (second load cycle north / south), clamping part bending proportions decreased significantly more: 38% -> 17% / 46% -> 32% (first load cycle north / south) and 36% -> 11% / 46% -> 27% (second load cycle).

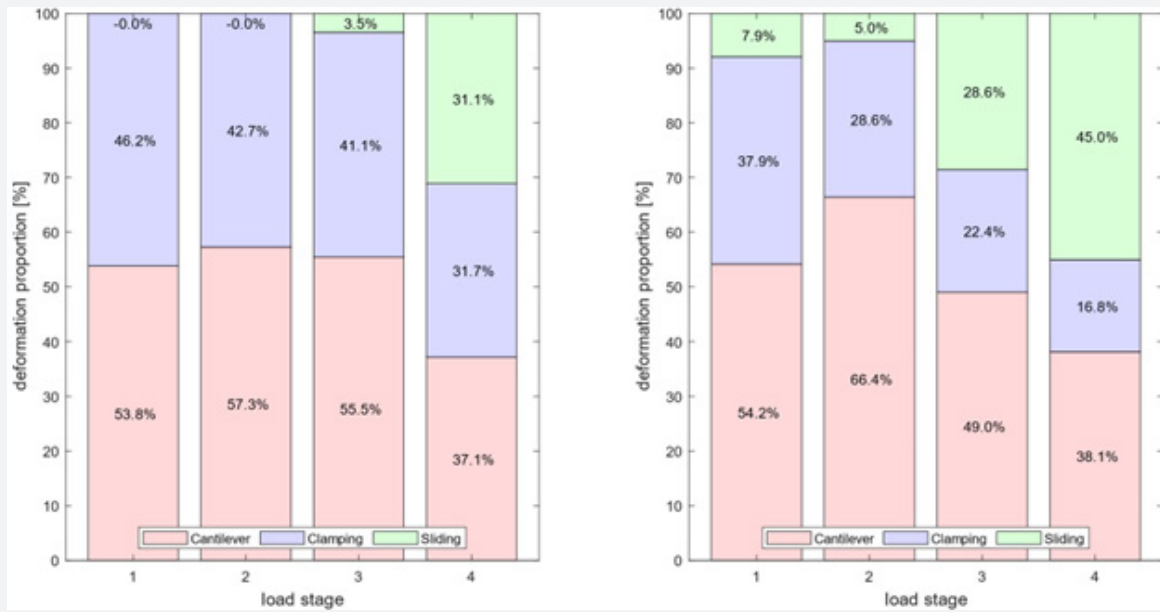


Figure 18: relative displacement components of Wall 2, first loading cycles: a) loading to south b) loading to north.

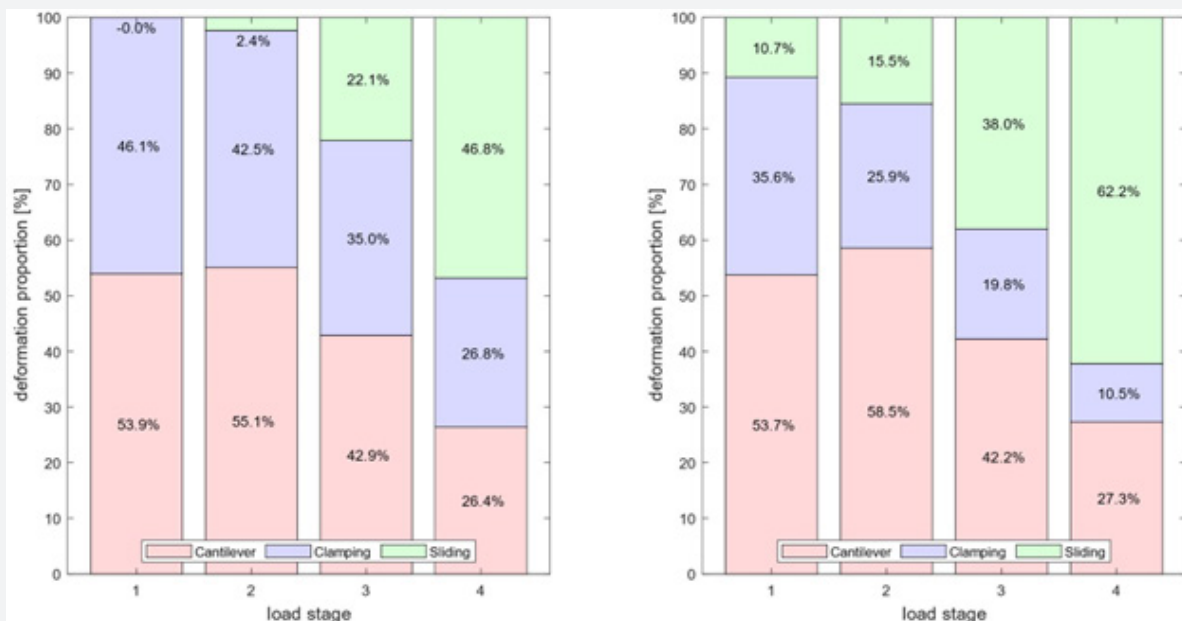


Figure 19: Relative displacement components of Wall 2, second loading cycles: a) loading to south b) loading to north.

A highly differentiated behavior occurred in Wall 4 (Figure 20 & Figure 21). With south loading, clamping part bending proportion was between 50% and 58%; for north loading, this proportion varied between 10% and 57%. Sliding shear component also varied greatly across the load stages and load

cycles. A small sliding shear component occurred in all cycles in the south direction ($\leq 14\%$). However, the main component leading to failure occurred in the north direction (42%) in the second cycle of load level 2, although almost no sliding shear was seen in this direction before.

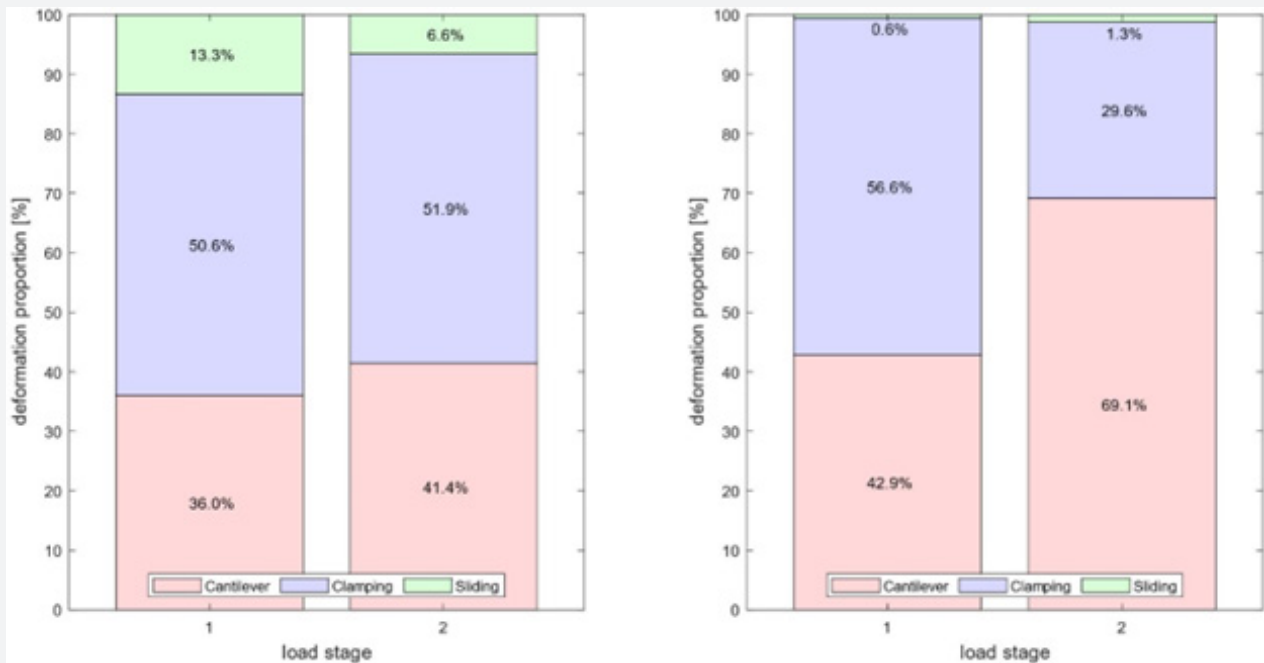


Figure 20: Relative displacement components of Wall 4, first loading cycles: a) loading to south b) loading to north.

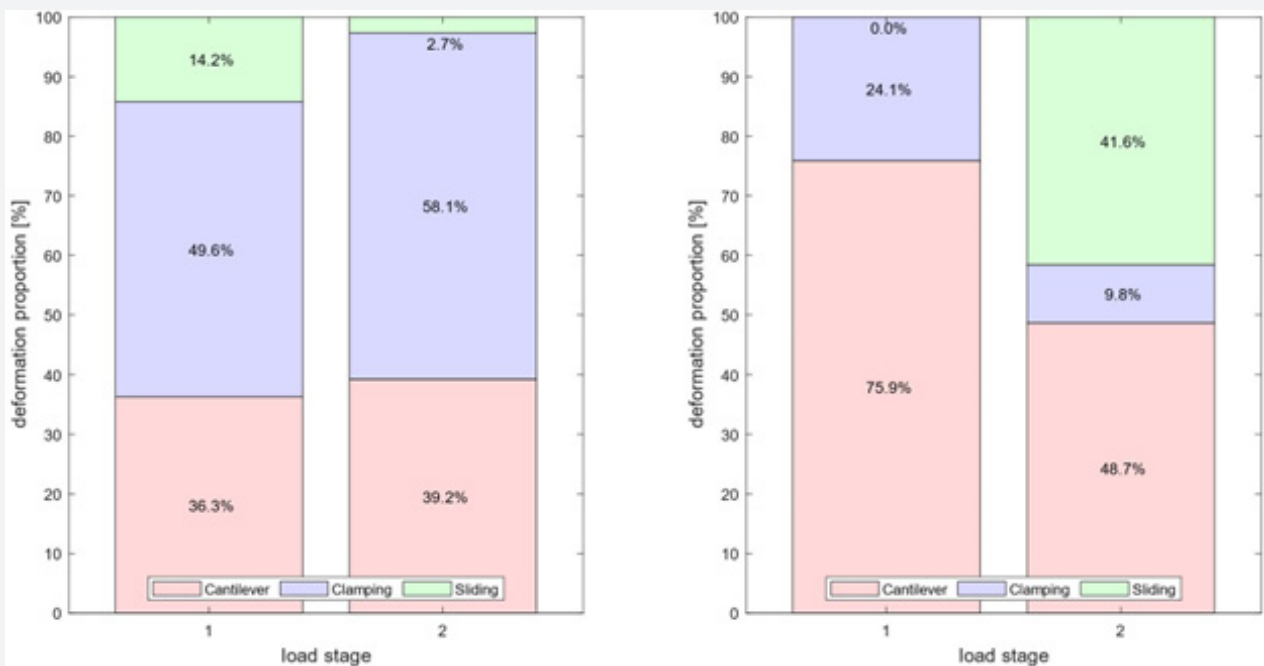


Figure 21: Relative displacement components of Wall 4, second loading cycles: a) loading to south b) loading to north.

Summary and Conclusion

Three reinforced concrete walls' load-deformation behavior was examined, including cantilever bending and clamping part deformation components and sliding at the construction joint below the basement ceiling. With selected geometric parameters and reinforcement layouts, representative cases from practice were investigated, with the following conclusions.

Crack Patterns

Particularly for Wall 1 and Wall 2, the later type of failure based on the crack pattern could already be predicted - or at least guessed - during the tests. Wall 1 (existing wall with small reinforcement ratio), which failed in bending, showed an almost exclusively horizontal crack pattern, where crack inclination only occurred near the neutral axis. Wall 2's crack pattern (earthquake-designed shear wall with reinforced boundaries) was characterized by inclined cracks, completely between the cantilever section end zones and over the total length of the clamped section. The crack patterns were caused by the higher shear forces and included the crack which was later responsible for the sliding shear failure. A bending crack opened in the construction joint below the ceiling cutout, which led to sliding displacements up to failure. In Wall 4 (squat wall), the crack pattern was less pronounced; already in cycle 2 of load stage 2, sliding shear failure started. The crack distribution was unsymmetric due to the location of the vertical support, which was on the ceiling axis north side.

Total top displacement

As expected, the greatest force that could be applied, as well as the greatest overall deformation, were observed in the test wall with the greatest reinforcement amount (Wall 2). As also expected, the squatter wall (Wall 4) could absorb more force than the slender wall (Wall 1); however, it exhibited a smaller deformation capacity. All tests also showed that force level was smaller when the load was applied again. In the second load cycles, the forces were about 10% to 30% smaller than the first cycles.

Clamping Area Bending Deformation

The tests showed that bending in the clamping area accounted for a non-negligible proportion of the overall deformation; Percentages from the clamping section were between 14% and 57% of total deformation. This large proportion from the clamping section should be considered in a deformation-based analysis, as this allows use of the stiffening wall's full deformation capacity. If the clamping section bending part is not considered, this deformation component can be regarded as an additional deformation reserve of the stiffening wall.

Sliding Failure

A sliding shear failure of the stiffening walls was observed in two tests. It must be clearly stated that sliding shear failure cannot be neglected in an earthquake analysis when squat walls

are used to stiffen buildings against earthquakes. As load level increases, proportion of displacement from sliding shear in total displacement increases continuously and bending proportion stagnates, or even decreases. The walls are becoming softer with each cycle compared to the initial stiff behavior. As a result, the load-deformation behavior calculated using the classical approach does not match the actual behavior, which leads to incorrect or inaccurate predictions - mostly on the unsafe side - in earthquake analysis. The tests also showed that occurrence of a sliding shear failure was not solely dependent on the ratio of wall height to wall length in the clamping zone; other factors were also involved, e.g., the reinforcement amount. Wall 1 and Wall 2 had the same geometry, although sliding shear failure was only observed in Wall 2. The greater the flexural resistance, the greater the shear force for the same geometry, which made sliding shear failure more likely.

In summary, additional attention should be paid to the clamping zone in earthquake analysis when calculating load-deformation behavior of a reinforced concrete wall. On one hand, deformation in the clamping zone can contribute significantly to the overall deformation, which has a positive effect; on the other hand, sliding shear failure can occur in this area, which must be prevented to ensure the structure's horizontal stability over complete earthquake duration. This applies particularly to squat walls in the clamping zone. In further investigations, additional relevant influencing factors on sliding shear failure could be studied and design recommendations could be prepared.

References

1. Ryan H, Goldsworthy H, Lumantarna E (2018) Plastic Hinge Length for Lightly Reinforced Rectangular Concrete Walls. *J Earthq Eng* 22(8): 1447-1478.
2. Dazio A, Wenk T, Bachmann H (1999) Versuche an Stahlbetontragwänden unter zyklisch-statischer Einwirkung. Zürich: IBK report 239.
3. Dazio A, Beyer K, Bachmann H (2009) Quasi-static cyclic tests and plastic hinge analysis of RC structural walls. *Eng Struct* 31(7): 1556-1571.
4. Hannewald P, Bimschas M, Dazio A (2013) Quasi-static cyclic tests on RC bridge piers with detailing deficiencies. Zürich: IBK report 352.
5. Syngé AJ (1980) Ductility of squat shear walls. Christchurch: University of Canterbury, Department of Civil Engineering.
6. Luna B, Rivera J, Whittaker, A (2015) Seismic behavior of low-aspect-ratio reinforced concrete shear walls. *ACI Struct J* 112(5): 593-604.
7. Trost B, Schuler H, Stojadinovic B (2019) Sliding in Compression Zones of Reinforced Concrete Shear Walls: Behavior and Modeling. *ACI Struct J* 116(5): 3-16.
8. Schuler H, Trost B (2016) Sliding Shear Resistance of Squat Walls under Reverse Loading: Mechanical Model and Parametric Study. *ACI Struct J* 113(4): 711-721.
9. Park R (1988) Ductility evaluation from laboratory and analytical testing. Tokyo-Kyoto: Proceedings of Ninth World Conference on Earthquake Engineering.



This work is licensed under Creative Commons Attribution 4.0 License
DOI: [10.19080/CERJ.2024.15.555901](https://doi.org/10.19080/CERJ.2024.15.555901)

Your next submission with Juniper Publishers will reach you the below assets

- Quality Editorial service
- Swift Peer Review
- Reprints availability
- E-prints Service
- Manuscript Podcast for convenient understanding
- Global attainment for your research
- Manuscript accessibility in different formats

(Pdf, E-pub, Full Text, Audio)

- Unceasing customer service

Track the below URL for one-step submission

<https://juniperpublishers.com/online-submission.php>